MNISTRY OF EDUCATION AND TRAINING

VIETNAM ACADEMY OF SCIENCE AND TECHNOLOGY

GRADUATE UNIVERSITY OF SCIENCES AND TECHNOLOGY



Dao Minh Tien

STATIC AND DYNAMIC ANALYSIS OF MULTI-LAYER ORGANIC NANOPLATES CONSIDERING THE SIZE EFFECT

SUMMARY OF THE DOCTORAL DISSERTATION IN MECHANICAL ENGINEERING AND ENGINEERING MECHANICS

Major: Engineering Mechanics Code: 9520101

Hanoi - 2025

The work was completed at the Graduate University of Sciences and Technology, Vietnam Academy of Science and Technology.
Supervisors: Supervisor 1: Assoc, Prof., Dr. Do Van Thom, Military Technical Academy Supervisor 2: Assoc, Prof., Dr. Dao Nhu Mai, Graduate University of Sciences and Technology
Reviewer 1:
The thesis was defended before the Doctoral Thesis Evaluation Council at the University level, meeting at the Graduate University of Sciences and Technology, Vietnam Academy of Science and Technology at o'clock, date month

The thesis can be found at:

- 1. Library of the Graduate University of Sciences and Technology
- 2. National Library of Vietnam

INTRODUCTION

1. The urgency of the dissertation

Energy consumption is an indispensable requirement for social progress. In previous decades, to meet the ever-increasing demand for energy, humanity has extensively exploited and utilized various types of fossil fuels. However, these conventional energy sources are gradually being depleted, and their consequences have proven to be extremely devastating, leading to the degradation of the global living environment. For this reason, the demand for environmentally friendly and renewable energy sources has become exceedingly urgent. Fortunately, humankind has discovered methods to harness solar energy - one of the most promising renewable energy sources that is entirely non-polluting and inexhaustible. The simplest way to utilize this energy is by developing solar energy absorption panels that directly convert sunlight into other usable forms of energy (commonly known as solar cells). To optimize the efficiency of solar energy absorption and conversion into electricity, comprehensive and detailed investigations are required concerning various aspects such as material properties, mechanical behavior, and manufacturing technology. Among these aspects, the study of the mechanical response of multilayer organic nanoplates (which serve as structural components in solar cell applications) plays a crucial role.

Based on the aforementioned analysis, the dissertation addresses the research topic entitled: "Static and dynamic analysis of multi-layer organic nanoplates considering the size effect."

2. Objectives of the dissertation

This dissertation aims to investigate the static and dynamic responses of organic nanoplate structures subjected to static and dynamic loadings, based on the finite element method (FEM) in conjunction with the nonlocal elasticity theory.

3. Scope and subjects of the study

The subject of the study is the multilayer organic nanoplate subjected to both static and dynamic loads. The scope of the research covers three fundamental problems: the linear static bending problem, the free vibration problem, and the linear forced vibration problem of multilayer organic nanoplates.

4. Research methodology

The research methodology is based on the finite element method (FEM) formulated within the framework of nonlocal elasticity theory.

5. Scientific and practical significance of the dissertation

The analysis of the static and dynamic responses of multilayer organic nanoplates holds significant importance in the field of structural mechanics. The findings of this dissertation provide new contributions to the analysis and understanding of organic nanoplate structures. The obtained results can serve as valuable references for researchers, designers, and manufacturers engaged in the development and fabrication of organic nanoplate materials and structures.

6. Structure of the dissertation

The dissertation is composed of the Introduction, four main chapters, Conclusion, a list of the author's scientific publications, and the references.

CHAPTER 1. OVERVIEW OF THE RESEARCH PROBLEM

Chapter 1 (26 pages) presents a comprehensive overview of nanomaterials, including their fabrication technologies and applications. The chapter also provides a review of theoretical models and computational approaches used in the analysis of nanostructures in general, as well as a summary of existing research findings related to the mechanical behavior and analysis of nanostructural systems.

CHAPTER 2. THEORETICAL BASIS FOR THE ANALYSIS OF ORGANIC NANOPLATES CONSIDERING THE SIZE EFFECTS

2.1. Problem model and assumptions

The organic nanoplate is modeled as illustrated in Figure 2.1. The plate consists of five distinct material layers, each possessing different

mechanical properties.

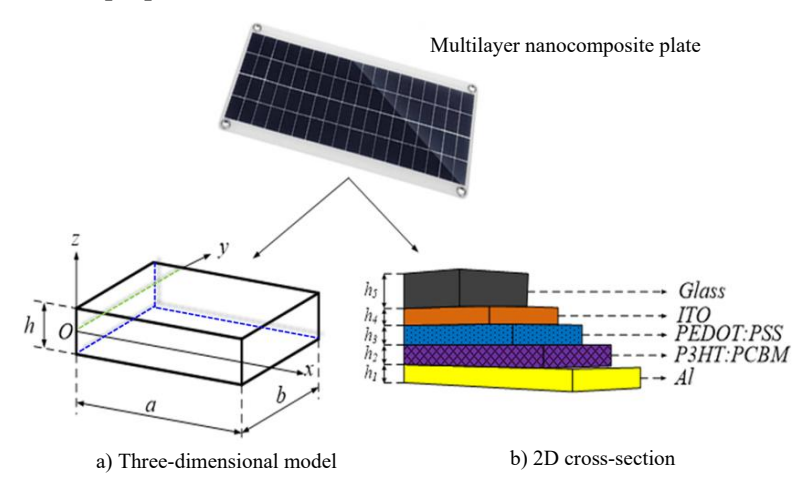


Figure 2.1. Model of the multilayer organic nanoplate

The dissertation adopts the following assumptions: The normal strain component ε_z =0. Small deformation assumptions are applied. Thermal effects are neglected. Each layer is considered linearly elastic.

2.2. Mechanical Behavior Relations of the Plate

The displacement field of the organic nanoplate [58, 87, 88]:

$$u(x, y, z) = -z \frac{\partial w_b}{\partial x} - f_z \frac{\partial w_s}{\partial x}; v(x, y, z) = -z \frac{\partial w_b}{\partial y} - f_z \frac{\partial w_s}{\partial y};$$

$$w(x, y, z) = w_b(x, y) + w_s(x, y)$$
(2.1)

where the function f_z can take one of the following three forms: The polynomial function is expressed as [87]: $f_z = -\frac{z}{4} + \frac{5}{3} \frac{z^3}{h^2}$; The sine function is expressed as [88]: $f_z = z - \frac{h}{\pi} \sin\left(\frac{\pi z}{h}\right)$; The hyperbolic sine function is expressed as [89]: $f_z = z - h \sinh\left(\frac{z}{h}\right) + z \cosh\left(\frac{1}{2}\right)$.

The strain field is given as follows:

$$\boldsymbol{\varepsilon} = \begin{cases} \varepsilon_{xx} \\ \varepsilon_{yy} \\ \varepsilon_{xy} \end{cases} = -z \begin{cases} \frac{\partial^2 w_b}{\partial x^2} \\ \frac{\partial^2 w_b}{\partial y^2} \\ 2\frac{\partial^2 w_b}{\partial x \partial y} \end{cases} - f_z \begin{cases} \frac{\partial^2 w_s}{\partial x^2} \\ \frac{\partial^2 w_s}{\partial y^2} \\ 2\frac{\partial^2 w_s}{\partial x \partial y} \end{cases} + g_z \begin{cases} 0 \\ 0 \\ 0 \end{cases}$$
 (2.5)

$$\boldsymbol{\varepsilon} = \left\{ \begin{matrix} \varepsilon_{xz} \\ \varepsilon_{yz} \end{matrix} \right\} = g_z \left\{ \begin{matrix} \frac{\partial w_s}{\partial x} \\ \frac{\partial w_s}{\partial y} \end{matrix} \right\}$$

The dissertation employs nonlocal elasticity theory; therefore, the constitutive relation between stress and strain in the *i-th* material layer is given by the following form [27], [89, 90]:

$$(1 - l^{2}\nabla^{2})\sigma^{i} = \begin{bmatrix} c_{11}^{i} & c_{12}^{i} & 0\\ c_{12}^{i} & c_{11}^{i} & 0\\ 0 & 0 & c_{33}^{i} \end{bmatrix} \begin{Bmatrix} \varepsilon_{x} \\ \varepsilon_{y} \\ \gamma_{xy} \end{Bmatrix}^{i} = D_{b}^{i}\varepsilon^{i} + \chi \frac{\partial \varepsilon^{i}}{\partial t} \quad (2.8)$$
$$(1 - l^{2}\nabla^{2})\tau^{i} = \begin{bmatrix} c_{33}^{i} & 0\\ 0 & c_{33}^{i} \end{bmatrix} \begin{Bmatrix} \gamma_{xz} \\ \gamma_{yz} \end{Bmatrix}^{i} = D_{s}^{i}\gamma_{s}^{i} + \chi \frac{\partial \gamma_{s}^{i}}{\partial t} \quad (2.9)$$

$$(1 - l^2 \nabla^2) \tau^i = \begin{bmatrix} c_{33}^i & 0 \\ 0 & c_{33}^i \end{bmatrix} \begin{Bmatrix} \gamma_{xz} \\ \gamma_{yz} \end{Bmatrix}^i = D_s^i \gamma_s^i + \chi \frac{\partial \gamma_s^i}{\partial t}$$
 (2.9)

where χ is the viscoelastic coefficient of the material.

To derive the equations of motion for the organic nanoplate, the dissertation employs the principle of minimum total potential energy [91]:

$$\delta U - \delta W - \delta T = 0 \tag{2.15}$$

where δU , δW and δT are the variations of the plate's strain potential energy, the work of external forces, and the kinetic energy variation.

After manipulation, the equilibrium equation of the nanoplate takes the following form:

$$\int_{\Omega} \left\{ \begin{bmatrix} -A_{z11} \frac{\partial^4 w_b}{\partial x^4} - B_{f11} \frac{\partial^4 w_s}{\partial x^4} - A_{z12} \frac{\partial^4 w_b}{\partial x^2 \partial y^2} - B_{f12} \frac{\partial^4 w_s}{\partial x^2 \partial y^2} \\ -\chi A_{z\chi} \frac{\partial}{\partial t} \left(\frac{\partial^4 w_b}{\partial x^4} + \frac{\partial^4 w_b}{\partial x^2 \partial y^2} + 2 \frac{\partial^4 w_b}{\partial x^2 \partial y^2} \right) - 4 A_{z33} \frac{\partial^4 w_b}{\partial x^2 \partial y^2} \\ -\chi B_{f\chi} \frac{\partial}{\partial t} \left(\frac{\partial^4 w_s}{\partial x^4} + \frac{\partial^4 w_s}{\partial x^2 \partial y^2} + 2 \frac{\partial^4 w_s}{\partial x^2 \partial y^2} \right) - 4 B_{f33} \frac{\partial^4 w_s}{\partial x^2 \partial y^2} \end{bmatrix} \right\} \delta w_b \right\} dx dy$$

$$+ \int_{\Omega} \begin{bmatrix} -B_{f11} \frac{\partial^4 w_b}{\partial x^4} - D_{f11} \frac{\partial^4 w_s}{\partial x^4} - B_{f12} \frac{\partial^4 w_b}{\partial x^2 \partial y^2} - D_{f12} \frac{\partial^4 w_s}{\partial x^2 \partial y^2} \\ -4 B_{f33} \frac{\partial^4 w_b}{\partial x^2 \partial y^2} - 4 D_{f33} \frac{\partial^4 w_s}{\partial x^2 \partial y^2} - \chi A_{s\chi} \left(\frac{\partial^4 w_s}{\partial x^4} + \frac{\partial^4 w_s}{\partial y^4} \right) \\ -\chi B_{f\chi} \frac{\partial}{\partial t} \left(\frac{\partial^4 w_b}{\partial x^4} + \frac{\partial^4 w_b}{\partial x^2 \partial y^2} + 2 \frac{\partial^4 w_b}{\partial x^2 \partial y^2} \right) \\ -\chi D_{f\chi} \frac{\partial}{\partial t} \left(\frac{\partial^4 w_s}{\partial x^4} + \frac{\partial^4 w_s}{\partial x^2 \partial y^2} + 2 \frac{\partial^4 w_s}{\partial x^2 \partial y^2} \right) \end{bmatrix} \right\} \delta w_s dx dy$$

$$-\int_{\Omega} \left\{ b_{x} \left[\delta w_{b} - \sum_{i} \frac{l_{i}^{2}h_{i}}{h} \left(\frac{\partial^{2}\delta w_{b}}{\partial x^{2}} \right) + p_{z} \left[-\sum_{i} \frac{l_{i}^{2}h_{i}}{h} \left(\frac{\partial^{2}\delta w_{s}}{\partial x^{2}} \right) \right] \right\} + p_{z} \left[-\sum_{i} \frac{l_{i}^{2}h_{i}}{h} \left(\frac{\partial^{2}\delta w_{s}}{\partial x^{2}} \right) \right] \right\} dxdy$$

$$-\left(\delta w_{b} + \delta w_{s} \right) \sum_{i} \frac{l_{i}^{2}h_{i}}{h} \left(\frac{\partial^{2}p_{z}}{\partial x^{2}} + \frac{\partial^{2}p_{z}}{\partial y^{2}} \right) + \left[-\left(\frac{\partial (\ddot{w}_{b} + \ddot{w}_{s}) \delta w_{b}}{\partial x} \right) + \left(\frac{\partial (\ddot{w}_{b} + \ddot{w}_{s}) \delta w_{b}}{\partial x} \right) + \left(\frac{\partial (\ddot{w}_{b} + \ddot{w}_{s}) \delta w_{b}}{\partial y} \right) \right] \right\} dxdy$$

$$-\int_{\Omega} \left\{ +\left\{ H_{1} \left(\frac{\partial^{2}\ddot{w}_{b}}{\partial x^{2}} + \frac{\partial^{2}\ddot{w}_{b}}{\partial y^{2}} \right) + H_{2} \left(\frac{\partial^{2}\ddot{w}_{s}}{\partial x^{2}} + \frac{\partial^{2}\ddot{w}_{s}}{\partial y^{2}} \right) \right\} \delta w_{b} + \left\{ H_{2} \left(\frac{\partial^{2}\ddot{w}_{b}}{\partial x^{2}} + \frac{\partial^{2}\ddot{w}_{b}}{\partial y^{2}} \right) + H_{3} \left(\frac{\partial^{2}\ddot{w}_{s}}{\partial x^{2}} + \frac{\partial^{2}\ddot{w}_{s}}{\partial y^{2}} \right) \right\} \delta w_{s} - \nabla^{2} \left\{ H_{2l} \left(\frac{\partial^{2}\ddot{w}_{b}}{\partial x^{2}} + \frac{\partial^{2}\ddot{w}_{b}}{\partial y^{2}} \right) + H_{3l} \left(\frac{\partial^{2}\ddot{w}_{s}}{\partial x^{2}} + \frac{\partial^{2}\ddot{w}_{s}}{\partial y^{2}} \right) \right\} \delta w_{s} - \nabla^{2} \left\{ H_{2l} \left(\frac{\partial^{2}\ddot{w}_{b}}{\partial x^{2}} + \frac{\partial^{2}\ddot{w}_{b}}{\partial y^{2}} \right) + H_{3l} \left(\frac{\partial^{2}\ddot{w}_{s}}{\partial x^{2}} + \frac{\partial^{2}\ddot{w}_{s}}{\partial y^{2}} \right) \right\} \delta w_{s} \right\}$$

2.3. Finite Element Model

The nanoplate is discretized into four-node quadrilateral elements (Figure 2.2), the nodal displacement vector is defined as follows:

$$q_e = \sum_{j=1}^{4} \left[w_{bj}, w_{sj}, \left(\frac{\partial w_b}{\partial x} \right)_j, \left(\frac{\partial w_s}{\partial x} \right)_j, \left(\frac{\partial w_b}{\partial y} \right)_j, \left(\frac{\partial w_s}{\partial y} \right)_j \right]$$

The variational formulation of the elastic strain potential energy is expressed as follows: $\delta U_e = q_e^T K_e \delta q_e + \dot{q}_e^T C_e \delta q_e$ (2.57) where the element stiffness matrix is given by:

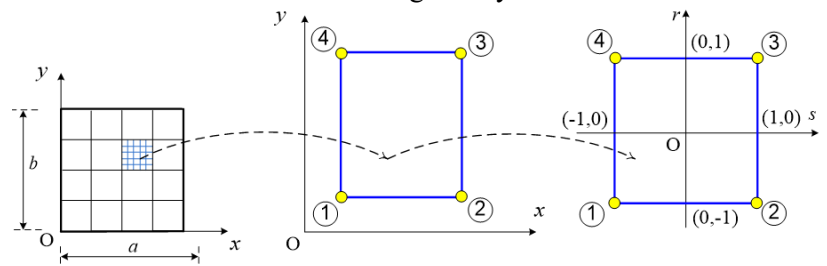


Figure 2.2. Representation of the Four-Node Quadrilateral Element.

$$K_e = K_e^b + K_e^s (2.58)$$

where:
$$K_e^b = \int_{\Omega_e} \left(\begin{bmatrix} V_z^T & V_f^T \end{bmatrix} \begin{bmatrix} A_z & B_f \\ B_f & D_f \end{bmatrix} \begin{bmatrix} V_z \\ V_f \end{bmatrix} \right) dxdy$$
 (2.59)

$$K_e^s = \int_{\Omega_\rho} (V_s^T A_s V_s) \, dx dy \tag{2.60}$$

And the element damping matrix of the plate, accounting for the viscoelastic behavior of the material, is expressed as follows:

$$C_e = \chi \int_{\Omega_e} \left(\begin{bmatrix} V_z^T & V_f^T \end{bmatrix} \begin{bmatrix} A_{z\chi} & B_{f\chi} \\ B_{f\chi} & D_{f\chi} \end{bmatrix} \begin{bmatrix} V_z \\ V_f \end{bmatrix} + \left(V_s^T A_{s\chi} V_s \right) \right) dx dy \quad (2.62)$$

The variational formulation of the kinetic energy is expressed as follows:

$$\delta T_e = \ddot{q}_e^T M_e \delta q_e \tag{2.69}$$

where the element mass matrix M_e is determined as follows:

$$M_{e} = \begin{bmatrix} \frac{\partial F_{b}^{T}}{\partial x} H_{1} \frac{\partial F_{b}}{\partial x} + \frac{\partial F_{b}^{T}}{\partial x} H_{2} \frac{\partial F_{s}}{\partial x} \\ + \frac{\partial F_{s}^{T}}{\partial x} H_{2} \frac{\partial F_{b}}{\partial x} + \frac{\partial F_{b}^{T}}{\partial x} H_{3} \frac{\partial F_{s}}{\partial x} \\ \frac{\partial F_{b}^{T}}{\partial y} H_{1} \frac{\partial F_{b}}{\partial y} + \frac{\partial F_{b}^{T}}{\partial y} H_{2} \frac{\partial F_{s}}{\partial y} \\ + \frac{\partial F_{s}^{T}}{\partial y} H_{2} \frac{\partial F_{b}}{\partial y} + \frac{\partial F_{s}^{T}}{\partial y} H_{3} \frac{\partial F_{s}}{\partial y} \\ F_{b}^{T} H_{0} F_{b} + F_{b}^{T} H_{0} F_{s} \\ + F_{s}^{T} H_{0} F_{b} + F_{s}^{T} H_{0} F_{s} \end{bmatrix}$$

$$(2.70)$$

From the variational expression of the external work, the dissertation derives the nodal load vector of the element as follows:

$$P_{e} = \int_{\Omega_{e}} \left\{ (F_{b} + F_{s})^{T} p_{z} l^{2} \begin{bmatrix} p_{z} \left(\frac{\partial^{2} (F_{b} + F_{s})^{T}}{\partial x^{2}} \right) \\ + \frac{\partial^{2} (F_{b} + F_{s})^{T}}{\partial y^{2}} \right) \\ + (F_{b} + F_{s})^{T} \left(\frac{\partial^{2} p_{z}}{\partial x^{2}} + \frac{\partial^{2} p_{z}}{\partial y^{2}} \right) \end{bmatrix} \right\} dx dy \quad (2.74)$$

After assembling the element mass matrices, element stiffness matrices, and element nodal force vectors, the equation of motion of the organic nanoplate: $M. \ddot{q} + C\dot{q} + K. q = P$ (2.78) where $M = \sum_e M_e$, $C = \sum_e C_e$, $K = \sum_e K_e$, and $P = \sum_e P_e$ are the global mass matrix, global damping matrix, global stiffness matrix, and global nodal load vector, respectively; while $\ddot{q} = \sum_e \ddot{q}_e$, $\dot{q} = \sum_e \dot{q}_e$, and $q = \sum_e q_e$

are the global nodal acceleration vector, global nodal velocity vector, and global nodal displacement vector of the organic nanoplate.

2.4. Boundary conditions

The plate is analyzed under different types of boundary constraints, including simply supported (denoted as S) and clamped (denoted as C) conditions. The specific boundary conditions for each case, considering a rectangular plate, are defined as follows:

- For a simply supported plate at x = 0 and x = a, the boundary conditions are:

$$w_{bi} = 0, w_{si} = 0, \left(\frac{\partial w_b}{\partial y}\right)_i = 0, \left(\frac{\partial w_s}{\partial y}\right)_i = 0$$
 (2.79)

- For a simply supported plate at y = 0 and y = b, the boundary conditions are:

$$w_{bi} = 0, w_{si} = 0, \left(\frac{\partial w_b}{\partial x}\right)_i = 0, \left(\frac{\partial w_s}{\partial x}\right)_i = 0$$
 (2.80)

- For a clamped plate at x = 0 and x = a, the boundary conditions are:

$$w_{bi} = 0, w_{si} = 0, \left(\frac{\partial w_b}{\partial x}\right)_i = 0, \left(\frac{\partial w_s}{\partial x}\right)_i, \left(\frac{\partial w_b}{\partial y}\right)_i = 0, \left(\frac{\partial w_s}{\partial y}\right)_i = 0$$
 (2.81)

- For a clamped plate at y = 0 and y = b, the boundary conditions are:

$$w_{bi} = 0, w_{si} = 0, \left(\frac{\partial w_b}{\partial x}\right)_i = 0, \left(\frac{\partial w_s}{\partial x}\right)_i, \left(\frac{\partial w_b}{\partial y}\right)_i = 0, \left(\frac{\partial w_s}{\partial y}\right)_i = 0 \quad (2.82)$$

2.5. Conclusions of Chapter 2

Based on the refined shear deformation theory, nonlocal elasticity theory, and the finite element method, the author has successfully established the stiffness matrix, mass matrix, and nodal force vector of the plate. Using the principle of minimum total potential energy, the equations of motion for the organic nanoplate under both static and dynamic loads have been formulated.

This chapter also defines the specific boundary conditions for various support configurations.

The mechanical behavior relations and the formulas presented in Chapter 2 have been published by the author in Articles 1–5 (see the author's list of publications).

CHAPTER 3. STATIC ANALYSIS OF ORGANIC NANOPLATES CONSIDERING THE SIZE EFFECTS AND INVESTIGATION OF THE INFLUENCE OF SEVERAL FACTORS

3.1. Finite element algorithm for solving the static bending problem of

the organic nanoplate

The equilibrium equation for an organic nanoplate subjected to static loading is expressed as follows: $K \cdot q = P$ (3.1)

From equation (3.1), the global nodal displacement vector of the plate can be determined as follows: $q = K^{-1}P$ (3.2)

The flowchart for solving the static bending problem of the organic nanoplate is shown in Figure 3.1. Based on the algorithm described above, the author developed the Solar_Nonlocal_Static_2025 (SNS_2025) program in the Matlab environment for the static analysis of organic nanoplates. The program consists of three main modules: Input and mesh generation module. Static analysis solver module for the organic nanoplate. Results output module.

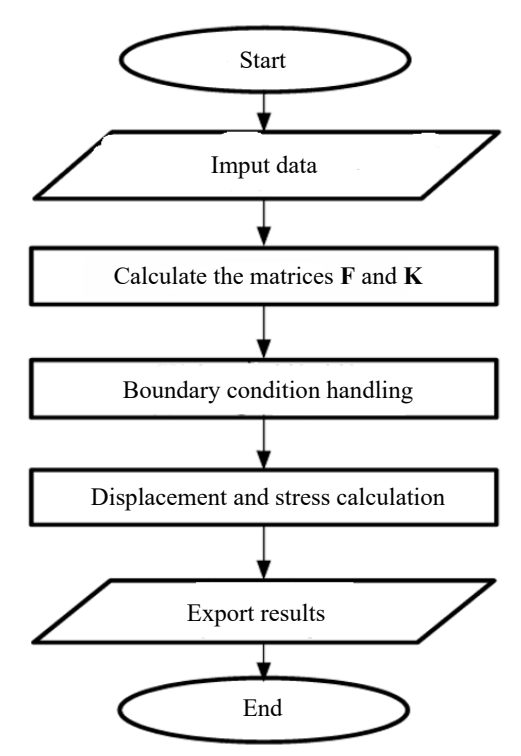


Figure 3.1. Flowchart for Solving the Static Bending Problem of the Organic NanoPlate.

3.2. Verification of the computational program

This section presents several examples to verify the accuracy of both the theoretical model and the computational program, using analytical solutions as well as the finite element method. The Navier-type solution of equation (2.43) is expressed as follows:

$$w_b(x,y) = \sum_{m=1}^{\infty} \sum_{n=1}^{\infty} W_{bmn} \sin\left(\frac{m\pi x}{a}\right) \sin\left(\frac{n\pi y}{b}\right)$$

$$w_s(x,y) = \sum_{m=1}^{\infty} \sum_{n=1}^{\infty} W_{smn} \sin\left(\frac{m\pi x}{a}\right) \sin\left(\frac{n\pi y}{b}\right)$$
(3.3)

where m and n are natural numbers, and W_{bmn} , W_{smn} are the amplitudes of the corresponding displacements. The load acting on the plate with amplitude P_{max} is defined by the following expression:

$$p_z(x,y) = \sum_{m=1}^{\infty} \sum_{m=1}^{\infty} \frac{16P_{max}}{\pi^2 mn} \sin\left(\frac{m\pi x}{a}\right) \sin\left(\frac{n\pi y}{b}\right)$$
(3.4)

Substituting expressions (3.3) and (3.4) into (2.43) yields a system of equations containing only the two unknowns W_{bmn} and W_{smn} , as follows:

$$\begin{bmatrix} K_{11} & K_{12} \\ K_{21} & K_{22} \end{bmatrix} \begin{Bmatrix} W_{bmn} \\ W_{smn} \end{Bmatrix} = \begin{Bmatrix} P_b \\ P_s \end{Bmatrix}$$
 (3.5)

Solving equation (3.5) yields the amplitudes W_{bmn} and W_{smn} :

$${W_{bmn} \brace W_{smn}} = \begin{bmatrix} K_{11} & K_{12} \\ K_{21} & K_{22} \end{bmatrix}^{-1} {P_b \brace P_s}$$
 (3.7)

By substituting equation (3.7) into expression (3.3), the static bending displacement can be obtained.

Verification example 1: This example compares the static bending displacement of the nanoplate accounting for the size effect via the nonlocal parameter l. The plate has a=b=10 nm, thickness hvarying from a/10 to a/100, E=30 MPa, $\nu=0.3$, $\rho=1$, uniformly distributed load $Q_0=1$, and is simply supported on all edges.

The maximum dimensionless displacement is calculated by the following formula $\tilde{w} = 10^3 h^3 w_{\text{max}} / \left(12\left(1-v^2\right)Q_0a^4\right)$. Table 3.1 presents the convergence of the finite element method (FEM) results for the static bending displacement of the nanoplate as the mesh density is gradually increased, considering different nonlocal elasticity parameters. The results in this table demonstrate that as the number of elements in the mesh increases,

the computed displacements of the nanoplate converge. A 16×16 element mesh provides the necessary accuracy when compared with the analytical solution based on the third-order shear deformation theory reported in reference [45]. Therefore, this mesh configuration will be used for all subsequent calculations.

Table 3.2 presents the comparison of the maximum displacements for different nonlocal parameters and plate thicknesses. The results demonstrate that the finite element method (FEM) computations are in close agreement with the analytical solutions and also consistent with the results reported in reference [45]. The slight discrepancies arise because the theoretical model in [45] is based on the third-order shear deformation theory, whereas the displacement field in this dissertation is formulated using the refined shear deformation theory.

Table 3.1. Convergence of the maximum dimensionless displacement \vec{w} of the nanoplate under static loading, a/h = 10, [45] using the third-order shear deformation theory.

1	Results of the dissertation using the finite element method with different mesh discretizations							
(nm)	6×6	10×10	14×14	16×16	18×18	20×20	[45]	
		f_z is	a polyno	mial funct	tion			
0	4.394	4.314	4.292	4.287	4.283	4.281	4.185	
0.5	4.583	4.506	4.484	4.478	4.475	4.472	4.560	
1	5.151	5.081	5.059	5.053	5.049	5.046	4.936	
			f_z is a sine	function				
0	4.393	4.313	4.292	4.286	4.283	4.280	4.185	
0.5	4.583	4.505	4.483	4.478	4.474	4.472	4.560	
1	5.152	5.081	5.058	5.052	5.049	5.046	4.936	
		f_z is	a hyperbo	olic sine fi	unction			
0	4.394	4.314	4.292	4.287	4.283	4.281	4.185	
0.5	4.583	4.506	4.484	4.478	4.475	4.472	4.560	
1	5.151	5.081	5.059	5.053	5.049	5.046	4.936	

Table 3.2. Comparison of the dimensionless displacement \vec{w} of the nanoplate with analytical results [45] using the third-order shear deformation theory.

			The diss	sertation			Analytical			
l (nm)	LA1	LA2	LA3	LA4	LA5	LA6	results [45]			
	a/h=10									
0	4.261	4.261	4.261	4.287	4.286	4.287	4.185			
0.5	4.447	4.446	4.447	4.478	4.478	4.478	4.560			
1	5.004	5.003	5.004	5.053	5.052	5.053	4.936			
	1		a/h	=50						
0	4.063	4.063	4.063	4.085	5 4.085	4.085	4.015			
0.5	4.244	4.244	4.244	4.269	4.269	4.269	4.377			
1	4.786	4.786	4.786	4.823	3 4.823	4.823	4.740			
	a/h=100									
0	4.057	4.057	4.057	4.078	3 4.078	4.078	4.010			
0.5	4.237	4.237	4.237	4.263	3 4.263	4.263	4.372			
1	4.779	4.779	4.779	4.816	4.816	4.816	4.734			

Note: LA1: Analytical solution with f_z as a polynomial function; LA2: Analytical solution with f_z as a sine function; LA3: Analytical solution with f_z as a hyperbolic sine function; LA4: FEM solution with f_z as a polynomial function; LA5: FEM solution with f_z as a sine function; LA6: FEM solution with f_z as a hyperbolic sine function.

3.3. Investigation of the effects of various parameters on the static bending response of organic nanoplates

The nanoplate has geometric parameters a, b, and h. The aspect ratio a/b varies from 1 to 4, and the thickness ratio a/h varies from 10 to 50. The plate is composed of five material layers with a total thickness h = 0.55044 nm; the individual layer thicknesses h_i are distributed proportionally as 550:0.120:0.050:0.170:0.100. The mechanical properties of each layer are given in Table 3.5. The plate is subjected to a uniformly distributed load of intensity P_{max} .

Table 3.5. Mechanical properties of each material layer [48]

Layer	Name	Elastic	Poisson's	Density
order	Name	modulus (GPa)	ratio	(kg/m^3)
1	Glass	69	0.23	2400

2	ITO	116	0.35	7120
3	PEDOT:PSS	2.3	0.4	1000
4	P3HT:PCBM	6	0.23	1200
5	Aluminum	70	0.35	2601

The two parameters at the midpoint of the plate:

$$w^* = \frac{10h_0^3 E_{glass}}{P_{max}a^4} w \left(x = \frac{a}{2}, y = \frac{b}{2} \right); \sigma_x^* = \frac{h_0}{P_{max}a} \sigma_x \left(x = \frac{a}{2}, y = \frac{b}{2}, z = \frac{h}{2} \right), \text{ where }$$

 $h_0 = 1$ nm. The formula for calculating this difference is expressed as follows:

$$Diff_{w} = \frac{w^{*}(l_{i} \neq 0)}{w^{*}(l_{i} = 0)}; Diff_{\sigma} = \frac{\sigma_{x}^{*}(l_{i} \neq 0)}{\sigma_{x}^{*}(l_{i} = 0)}; Diff_{\omega} = \frac{\omega_{i}^{*}(l_{i} \neq 0)}{\omega_{i}^{*}(l_{i} = 0)}$$
(3.9)

- Effect of plate thickness and nonlocal elastic parameter

The dissertation assigns the nonlocal parameter of each layer l_i to vary from 0 to $2h_i$, and the plate length-to-thickness ratio a/h varies from 10 to 50. The computational results are presented in Tables 3.6 and 3.7.

- + If the nonlocal elastic parameter l_i increases, both the displacement and the stress of the organic nanoplate increase, which indicates that the nonlocal parameter effectively reduces the stiffness of the nanoplate.
- + The results obtained by both analytical methods and the finite element method, across the three plate theories considered, are similar, indicating that either analytical or numerical approaches may be used to solve the bending problem of organic nanoplates.

Figure 3.2 is the plot showing the differences in displacement and stress as functions of the ratio l_i/h_i for three values of the thickness ratio a/h. When a/h=10, the discrepancy in displacement and stress (between the cases with and without the nonlocal parameter l_i) becomes more pronounced as l_i/h_i increases. However, for a/h=50 the discrepancy between the two cases is not evident (the maximum discrepancy of displacement does not exceed 3% for $l_i/h_i=2$), which implies that if very high accuracy is not required, the effect of the nonlocal elastic parameter may be neglected, considerably simplifying the computations.

Table 3.6. Dimensionless bending displacement w^* depending on the ratio a/h and the nonlocal parameter l_i .

l_i/h_i	0	0.2	0.5	1.0	1.5	2.0				
	a = 10h									
LA1	2.9347	2.9552	3.0625	3.4458	4.0847	4.9791				
LA2	2.9345	2.9550	3.0623	3.4456	4.0845	4.9788				
LA3	2.9347	2.9552	3.0625	3.4458	4.0847	4.9791				
LA4	2.9068	2.9276	3.0365	3.4257	4.0742	4.9822				
LA5	2.9066	2.9273	3.0363	3.4253	4.0737	4.9815				
LA6	2.9068	2.9276	3.0365	3.4257	4.0742	4.9822				
			a = 20h							
LA1	2.8375	2.8425	2.8689	2.9629	3.1196	3.3389				
LA2	2.8375	2.8425	2.8688	2.9628	3.1195	3.3389				
LA3	2.8375	2.8425	2.8689	2.9629	3.1196	3.3389				
LA4	2.8091	2.8141	2.8406	2.9354	3.0933	3.3144				
LA5	2.8090	2.8141	2.8406	2.9354	3.0933	3.3144				
LA6	2.8091	2.8141	2.8406	2.9354	3.0933	3.3144				

Table 3.7. Dimensionless stress σ_x^* as a function of the ratio a/h and the nonlocal elastic parameter l_i .

l_i/h_i	0	0.2	0.5	1.0	1.5				
	a = 10h								
LA1	4.8630	4.8818	4.9804	5.3327	5.9200				
LA2	4.8643	4.8831	4.9816	5.3333	5.9196				
LA3	4.8628	4.8816	4.9803	5.3327	5.9200				
LA4	4.9602	4.9868	5.1267	5.6263	6.4590				
LA5	4.9621	4.9887	5.1287	5.6285	6.4615				
LA6	4.9600	4.9867	5.1265	5.6261	6.4587				
		а	=20h						
LA1	9.6945	9.7041	9.7544	9.9340	10.2334				
LA2	9.6952	9.7048	9.7550	9.9346	10.2339				
LA3	9.6945	9.7040	9.7543	9.9340	10.2334				
LA4	9.8771	9.8902	9.9593	10.2059	10.6170				

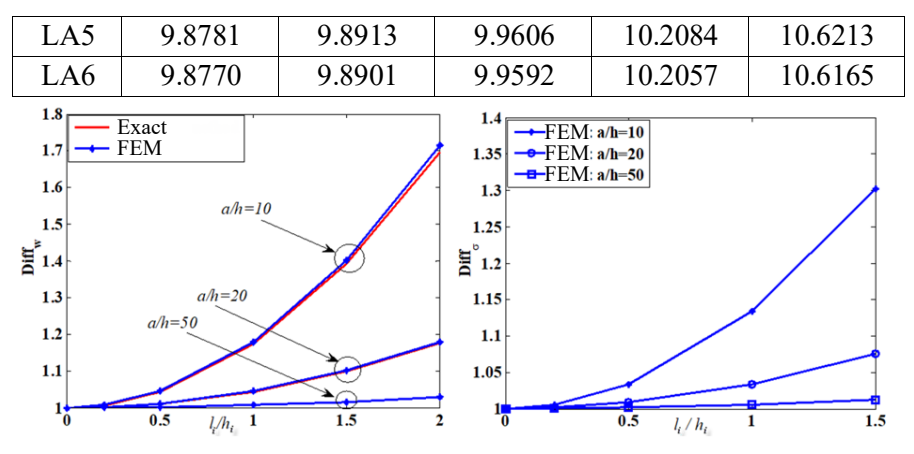


Figure 3.2. Graphs illustrating the variation of displacement and stress errors with respect to l_i/h_i , f_z is a polynomial function

- Effect of length ratio b/a and nonlocal elastic parameter

Tables 3.8 and 3.9 present the displacement and stress of the organic nanoplates for different values of the side length ratio b/a and the ratio l_i/h_i . The computational results show that:

For different values of the ratio b/a, as the nonlocal elastic parameter l_i increases, the deviation in the displacement and stress of the organic nanoplate compared with the classical theory becomes more significant. This further confirms that the effect of the nonlocal elastic parameter cannot be neglected in the analysis of organic nanoplates. The computational results obtained by the finite element method and the analytical method based on all three shear deformation theories are in very good agreement.

Figure 3.3 presents the calculated differences in stress and displacement with respect to the ratio l_i/h_i . These differences increase as the nonlocal elastic parameter l_i increases, and decrease as the ratio b/a increases.

Table 3.8. The dimensionless deflection w^* of the nanoplate depending on the ratio b/a, with a/h = 10.

l_i/h_i	0	0.2	0.5	1.0	1.5				
	b = a								
LA1	2.9347	2.9552	3.0625	3.4458	4.0847				
LA2	2.9345	2.9550	3.0623	3.4456	4.0845				

LA3	2.9347	2.9552	3.0625	3.4458	4.0847
LA4	2.9068	2.9276	3.0365	3.4257	4.0742
LA5	2.9066	2.9273	3.0363	3.4253	4.0737
LA6	2.9068	2.9276	3.0365	3.4257	4.0742

Table 3.9. Dimensionless stress σ_x^* as a function of the ratio b/a and the nonlocal elastic parameter l_i .

l_i/h_i	LA1	LA2	LA3	LA4	LA5	LA6				
	b = a									
1.5	5.9200	5.9196	5.9200	6.4590	6.4615	6.4587				
1.0	5.3327	5.3333	5.3327	5.6263	5.6285	5.6261				
0.5	4.9804	4.9816	4.9803	5.1267	5.1287	5.1265				
0.2	4.8818	4.8831	4.8816	4.9868	4.9887	4.9867				
0	4.8630	4.8643	4.8628	4.9602	4.9621	4.9600				

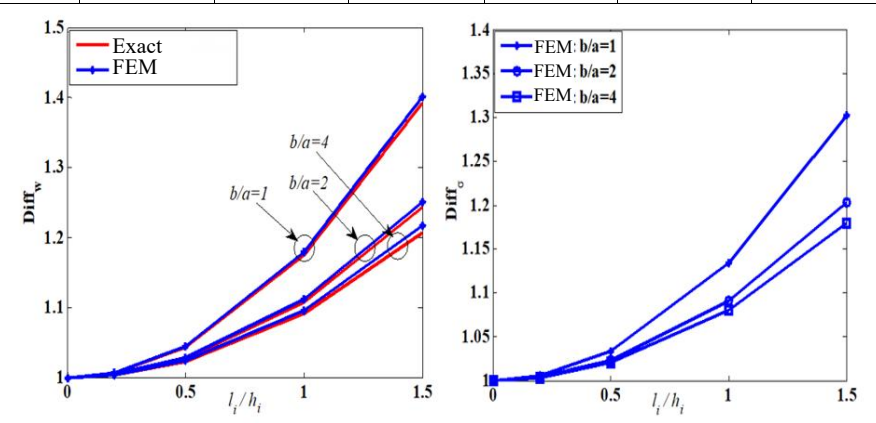


Figure 3.3. The graph illustrates the error of stress and deflection

3.5. Conclusions of Chapter 3

Chapter 3 has addressed the following main contents:

The author developed a finite element algorithm and the Solar_Nonlocal_Static_2025 (SNS_2025) program for analyzing organic nanoplates, taking into account the size-dependent effect. A Navier-type analytical solution was also presented to verify the finite element results. The finite element results were compared with analytical and published results, showing good accuracy and reliability.

The contents of this chapter have been published in Paper No. 1 (see the author's list of publications).

CHAPTER 4. DYNAMIC RESPONSE ANALYSIS OF ORGANIC NANOPLATES CONSIDERING THE SIZE EFFECT AND INVESTIGATION OF THE INFLUENCE OF SEVERAL PARAMETERS 4.1. Free vibration problem

The equation of motion for a free, undamped vibration of the plate is expressed as follows: $M\ddot{q} + Kq = 0$ (4.1)

To determine the natural frequencies and corresponding mode shapes of the organic nanoplate, assume a solution of the form $q = q_0 \sin(\omega t)$, where q_0 is the amplitude vector and ω is the angular frequency. Substituting this into the free undamped equation (4.1) yields the following eigenvalue problem: $(K - M\omega^2)q_0 = 0$ (4.2)

Equation (4.2) is a homogeneous linear system and admits a nontrivial solution $q_0 \neq 0$ if and only if the determinant of the matrix $(K - M\omega^2)$ vanishes, i.e. $\det(K - M\omega^2) = 0$ (4.3)

Solving equation (4.3) yields N natural frequencies ω_i of the structure. Corresponding to each natural frequency ω_i , substituting it into equation (4.2) gives the corresponding eigenvector q_i .

The algorithm diagram for solving the free vibration problem of the organic nanoplates is shown in Figure 4.1.

Based on the algorithm presented above, the author developed the computational program Solar Nonlocal Freevibration 2025 (SNF 2025).

For the free vibration problem, starting from equation (2.43), neglecting the right-hand side and ignoring damping, the dissertation adopts the Navier-type solution as follows:

$$w_b(x,y) = \sum_{m=1}^{\infty} \sum_{n=1}^{\infty} W_{bmn} \sin\left(\frac{m\pi x}{a}\right) \sin\left(\frac{n\pi y}{b}\right) e^{i\omega t}$$

$$w_s(x,y) = \sum_{m=1}^{\infty} \sum_{n=1}^{\infty} W_{smn} \sin\left(\frac{m\pi x}{a}\right) \sin\left(\frac{n\pi y}{b}\right) e^{i\omega t}$$
(4.4)

In which ω is the vibration frequency of the plate. Substituting expressions (4.4) into (2.43), we obtain the following system of equations:

$$\begin{bmatrix} K_{11} - M_{11} & K_{12} - M_{12} \\ K_{21} - M_{21} & K_{22} - M_{22} \end{bmatrix} \begin{Bmatrix} W_{bmn} \\ W_{smn} \end{Bmatrix} = \begin{Bmatrix} 0 \\ 0 \end{Bmatrix}$$
 (4.5)

By solving equation (4.5), the natural frequencies and corresponding mode shapes are obtained. The solution in this study employs the first three terms of the series.

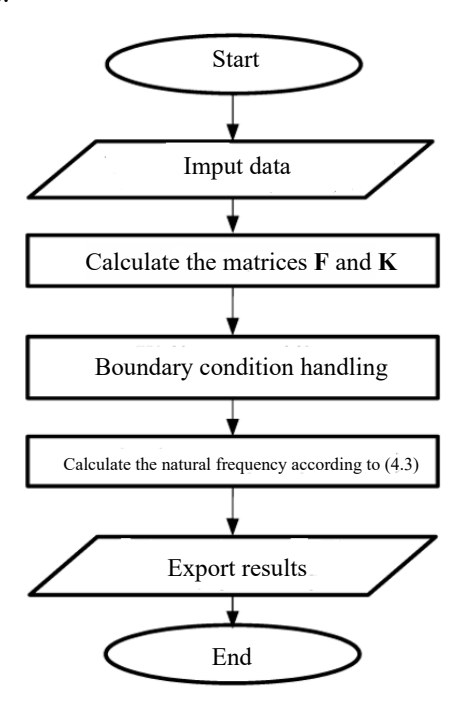


Figure 4.1. Algorithm diagram for solving the free vibration problem of the organic nanoplate.

Table 4.3 presents the calculated results for the first natural frequency of the organic nanoplates. From these data, it can be observed that as the ratio l_i/h_i increases, the natural frequency of the plate decreases. Figure 4.2 illustrates the difference in the first natural frequency between the cases with and without considering the effect of the nonlocal elasticity parameter. It is evident that as the plate becomes thinner (i.e., the a/h ratio increases), the difference in the first natural frequency between the two cases becomes smaller. For example, when a/h = 50, the difference between the two cases is less than 4%. Therefore, if high accuracy is not required, the effect of the

nonlocal parameter l_i can be neglected.

Table 4.3. The first natural frequency ω_1^* of the organic nanoplate as a function of a/h and the nonlocal elastic parameter, with b/a = 1, $\omega_1^* = \omega_1 h \sqrt{\rho_{glass} / E_{glass}}$

l_i/h_i	LA1	LA2	LA3	LA4	LA5	LA6				
	a=10h									
2.0	0.0430	0.0430	0.0430	0.0423	0.0423	0.0423				
1.5	0.0478	0.0478	0.0478	0.0471	0.0471	0.0471				
1.0	0.0525	0.0525	0.0525	0.0517	0.0517	0.0517				
0.5	0.0561	0.0561	0.0561	0.0552	0.0552	0.0552				
			a=20h	ı						
2.0	0.0133	0.0133	0.0133	0.0132	0.0132	0.0132				
1.5	0.0138	0.0138	0.0138	0.0137	0.0137	0.0137				
1.0	0.0142	0.0142	0.0142	0.0141	0.0141	0.0141				
0.5	0.0144	0.0144	0.0144	0.0144	0.0144	0.0144				

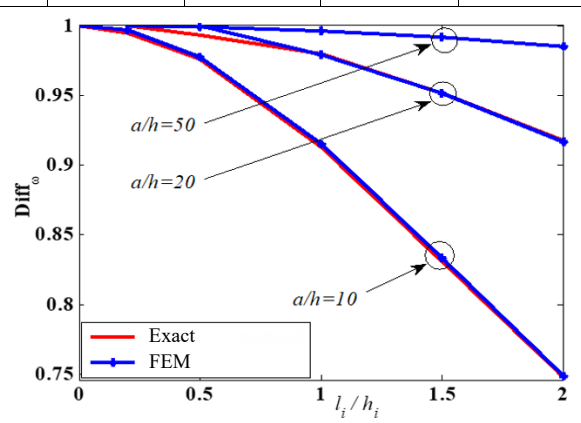


Figure 4.2. The difference in the first natural frequency between the cases considering and neglecting the size effect, where f_z is a polynomial function.

4.2. Forced vibration problem

The equation of forced vibration with damping for the organic nanoplates, as given in (2.78): $M\ddot{q} + C\dot{q} + Kq = F$ (4.7)

To solve equation (4.7), the thesis employs the Newmark direct integration method and develops the computational program

Solar_Nonlocal_Dynamic_2025 (SND_2025). The algorithm flowchart is shown in Figure 4.6. The plate is subjected to a uniformly distributed load varying according to the law: $p_z = P_0 \cdot F(t)$, where P_0 is the load amplitude:

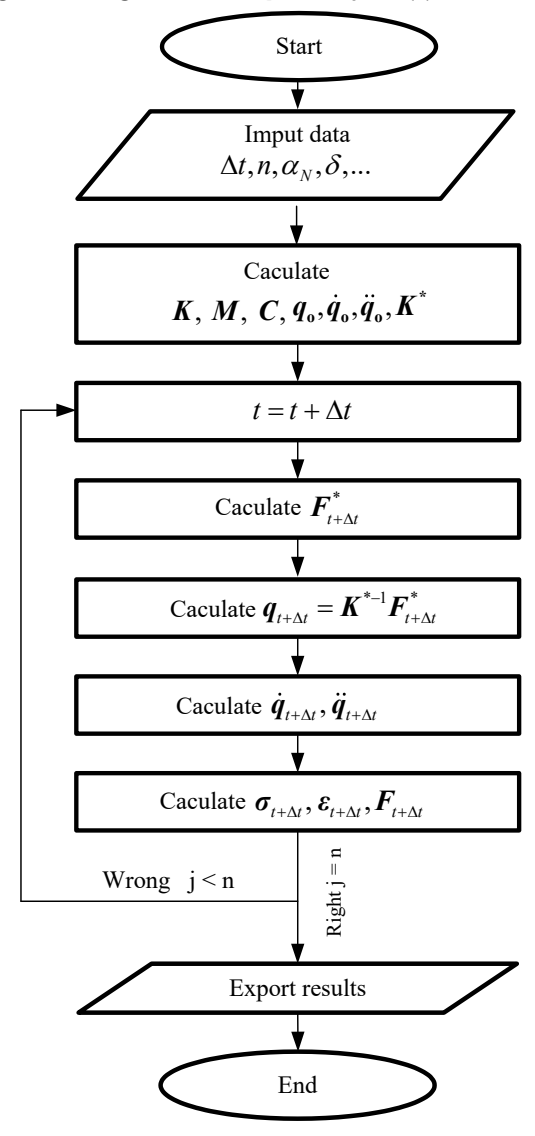


Figure 4.6. Algorithm diagram for solving the forced vibration problem of the organic nanoplate.

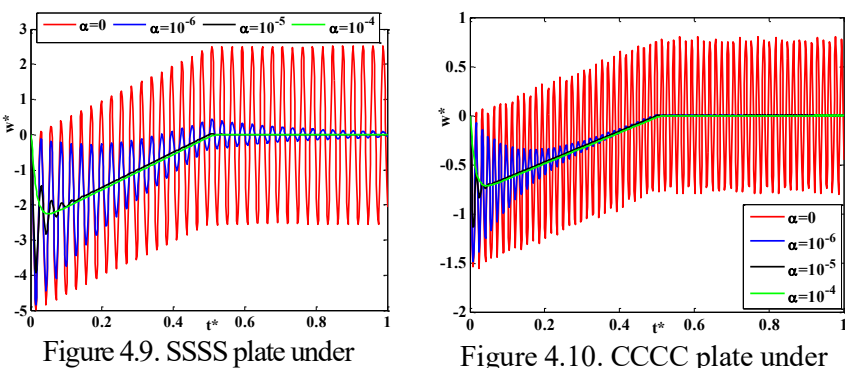
Sinusoidal load:
$$F(t) = \begin{cases} sin\left(\omega \frac{t}{t_1}\right) & 0 \le t \le t_1 \\ 0 & t > t_1 \end{cases}$$
; $t_1 = 5$ ms; Triangular load: $F(t) = \begin{cases} 1 - \frac{t}{t_1} & 0 \le t \le t_1 \\ 0 & t > t_1 \end{cases}$

The computational parameter is the displacement at the center of the plate: $w^* = \frac{E_{Al}h^3}{12P_0a_0^4}w\left(\frac{a}{2},\frac{b}{2}\right)$; $a_0 = 10h$. In the following computational results, the plate thickness h remains constant at h = 0.55044 nm, while in each example below, the plate side lengths a and b may vary. The damping parameter of the organic nanoplate is calculated using the dimensionless expression of the viscoelastic parameter $\alpha = \chi/E_{Al}$. In the general case, this damping parameter depends on the characteristics of each material type, and experimental testing is required to accurately determine this coefficient. However, to facilitate the computational process, the dissertation only considers the case where the damping parameter remains constant across all material layers, with its value ranging from 0 to 10^{-4} .

- Influence of the damping parameter

triangular loading

The variation of the mid-plane displacement over time corresponding to different values of the damping coefficient is shown in Figures 4.9 - 4.12. Some observations can be drawn as follows:

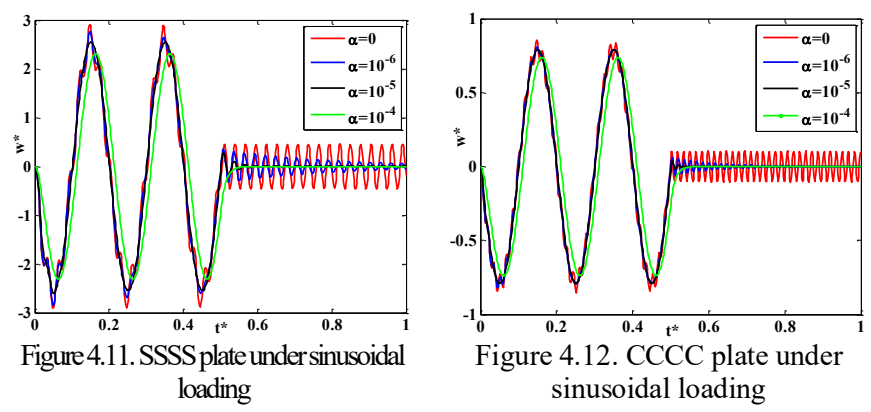


- In the case where damping is neglected, when the external force ceases, the plate continues to vibrate freely without decaying. However, when the structural damping is considered, the vibration of the plate

triangular loading.

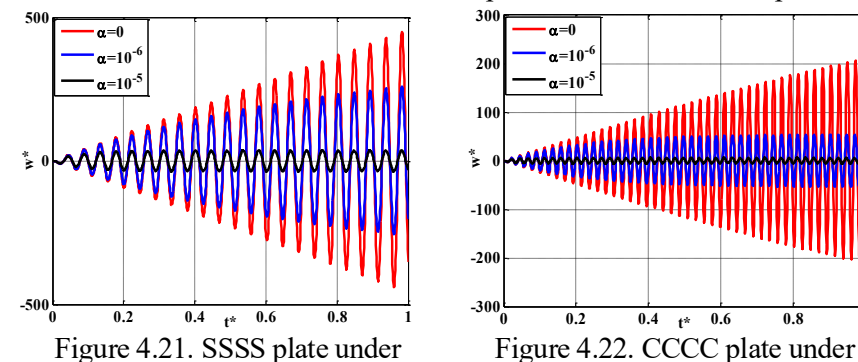
gradually diminishes after the external force is removed.

- During forced vibration (when the excitation force is still acting), the larger the damping coefficient, the smaller the maximum displacement of the plate. This is because part of the energy is dissipated through the structural damping.



- Influence of the loading frequency acting on the plate

When the frequency of the external force coincides with the natural frequency of the plate, the maximum displacement of the plate gradually increases over time-this is the resonance phenomenon in the nanoplate.



4.5. Conclusion of Chapter 4

sinusoidal loading

The results presented in Chapter 4 have addressed the following main points:

sinusoidal loading.

A computational program for analyzing the free vibration of organic nanoplates, Solar_Nonlocal_Freevibration_2025 (SNF_2025), has been developed. Verification with published results shows the program's reliability.

The dissertation has demonstrated the influence of the nonlocal elastic parameter and the plate thickness on the natural frequencies of organic nanoplates, using both the finite element method and analytical solutions. The results indicate that for thick plates (a/h=10), the effect of the nonlocal parameter is significant; however, for thin plates (a/h=50), this effect becomes negligible.

A computational program for analyzing the forced vibration of organic nanoplates under dynamic loading, Solar_Nonlocal_Dynamic_2025 (SND_2025), has also been developed, showing good accuracy and reliability.

The computational results in this chapter have been published in papers No. 1 and 2 (Author's publication list).

CONCLUSION

The dissertation has made the following significant new contributions:

- 1. A theoretical model has been established, and the equilibrium equations for organic nanoplates have been derived for the general case, as well as for the problems of static bending, free vibration, and forced vibration, taking into account small-scale effects.
- 2. By employing the Finite Element Method (FEM) in combination with nonlocal elasticity theory, the dissertation has developed algorithms to solve the problems of static bending, free vibration, and forced vibration of organic nanoplates considering the size effect. The results reveal clear differences between the nonlocal elasticity theory (which includes small-scale effects) and the classical elasticity theory (which neglects them).
- 3. A set of computational programs SNS_2025, SNF_2025, and SND_2025 has been developed to calculate deflections, stresses, natural frequencies, and forced displacements of five-layer organic nanoplates while accounting for the small-scale effect.
- 4. The effects of various parameters such as the nonlocal elasticity coefficient, geometric dimensions, damping ratio, boundary conditions, and excitation frequency on the static bending, free vibration, and forced vibration responses of organic nanoplates have been thoroughly investigated. The results show that the size effect becomes significant for thicker plates, whereas it diminishes as the plate becomes thinner.
 - 5. The numerical data obtained from this dissertation can serve as a

useful reference for the design of organic nanoplate structures subjected to static and dynamic loads, such as micro-scale energy storage devices, sensors, and electronic chips.

LIST OF PUBLISHED WORKS RELATED TO THE THESIS

- **1. Dao Minh Tien**, Do Van Thom, Phung Van Minh, Nguyen Chi Tho, Tran Ngoc Doan, Dao Nhu Mai (2023). The application of the nonlocal theory and various shear strain theories for bending and free vibration analysis of organic nanoplates. *Mechanics Based Design of Structures and Machines*, vol. 52 (1), pp. 588-610. https://doi.org/10.1080/15397734.2023.2186893. (ISI).
- **2. Dao Minh Tien**, Do Van Thom, Nguyen Thi Hai Van, Abdelouahed Tounsi, Phung Van Minh, Dao Nhu Mai, 2023, Buckling and forced oscillation of organic nanoplates taking the structural drag coefficient into account. *Computers and Concrete*, vol. 33 (1), pp. 91-102. https://doi.org/10.12989/cac.2024.33.1.091. (ISI).
- **3.** Nguyen Chi Tho, **Dao Minh Tien**, Do Van Thom, Phung Van Minh, Dao Van Doan (2024). A new approach to the static bending problem of organic nanoplates. *Part C: Journal of Mechanical Engineering Science*, vol. 239 (8), pp. 3052-3064. https://doi.org/10.1177/09544062241306986 (ISI).
- **4. Dao Minh Tien**, Nguyen Thi Cam Nhung, Do Van Thom, Ta Duc Tam (2023). Thermal buckling of organic nanoplates. The 7th International Conference on Engineering Mechanics and Automation (ICEMA 2023), Hanoi, November, 11÷12, 2023.
- **5. Dao Minh Tien**, Đỗ Văn Thom, Phùng Văn Minh, Phạm Huy Hiếu (2024). Bending and buckling responses of organic nanoplates considering the size effect. *Tạp chí Khoa học Giao thông vận tải*, số. 75(7), tr. 2015-2029. https://doi.org/10.47869/tcsi.75.7.1